The American Journal of Pathology, Vol. 175, No. 1, July 2009

DOI: 10.2353/ajpath.2009.080807

Neurobiology

Up-Regulation of Soluble Axl and Mer Receptor Tyrosine Kinases Negatively Correlates with Gas6 in Established Multiple Sclerosis Lesions

Jason G. Weinger,* Kakuri M. Omari,* Kurt Marsden,* Cedric S. Raine,*†‡ and Bridget Shafit-Zagardo*

From the Departments of Pathology, Neurology,† and Neuroscience,‡ Albert Einstein College of Medicine, Bronx, New York*

Multiple sclerosis is a disease that is characterized by inflammation, demyelination, and axonal damage; it ultimately forms gliotic scars and lesions that severely compromise the function of the central nervous system. Evidence has shown previously that altered growth factor receptor signaling contributes to lesion formation, impedes recovery, and plays a role in disease progression. Growth arrest-specific protein 6 (Gas6), the ligand for the TAM receptor tyrosine kinase family, consisting of Tyro3, Axl, and Mer, is important for cell growth, survival, and clearance of debris. In this study, we show that levels of membrane-bound Mer (205 kd), soluble Mer (~150 kd), and soluble Axl (80 kd) were all significantly elevated in homogenates from established multiple sclerosis lesions comprised of both chronic active and chronic silent lesions. Whereas in normal tissue Gas6 positively correlated with soluble Axl and Mer, there was a negative correlation between Gas6 and soluble Axl and Mer in established multiple sclerosis lesions. In addition, increased levels of soluble Axl and Mer were associated with increased levels of mature ADAM17, mature ADAM10, and Furin, proteins that are associated with Axl and Mer solubilization. Soluble Axl and Mer are both known to act as decoy receptors and block Gas6 binding to membrane-bound receptors. These data suggest that in multiple sclerosis lesions, dysregulation of protective Gas6 receptor signaling may prolong lesion activity. ***(Am J Pathol 2009, 175:283–293; DOI: 10.2353/ajpath.2009.080807)***

Multiple sclerosis (MS) is a debilitating white matter disease of the central nervous system (CNS). Although much of the evidence from animal models and MS suggests it to be an autoimmune disorder mediated by TH-1 type T cells,[1] other possible causes include genetic and environmental factors, antibody-dependent cytotoxicity, and bacterial and viral infections that may mediate altered protein expression resulting in inflammation, axonal and oligodendrocyte damage, demyelination and CNS scarring.[2] Growth and survival factors that protect against axonal and oligodendrocyte damage or loss, and dampen the inflammatory response are actively being pursued for MS therapy.[2–6] One growth factor associated with oligodendrocyte maturation, survival and dampening the immune response is growth-arrest specific protein 6 (Gas6). Gas6 is a secreted protein that is widely expressed in the central and peripheral nervous systems by endothelial cells and neurons, and is involved in numerous physiological and pathological functions including cell growth, survival and apoptosis.[7–12] Gas6 binds and activates the TAM family of receptor tyrosine kinases consisting of Tyro3 (Rse/Dtk/Sky), Axl (Ufo), and Mer (Eyk).[8,11,13,14,15] Many cell types express all three receptors and receptor activation can result from homophilic and heterophilic interactions.[16,17] Axl contains the major and minor Gas6 binding groove. Only the minor groove is conserved in Tyro3 and Mer and as a result, response to Gas6 is mediated in a concentration-dependent manner; Gas6 binding affinity is Axl>Tyro3>Mer.[18]

Supported by the National Multiple Sclerosis Society research grants RG3020 (to B.S.Z.) and RG4046 (to B.S.Z.), National Institutes of Health grant NINDS1R21NS061128 (to B.S.Z.), a, National Institutes of Health Training Program in Cellular and Molecular Biology and Genetics grant NIGMS GM07491 (to J.G.W.), National Multiple Sclerosis Society grant RG1001-K-11 (to C.S.R.), National Institutes of Health grant NS 08952 (to C.S.R.), and National Multiple Sclerosis Society fellowship FG1422-A-1 (to K.M.O.). C.S.R. is Wollowick Family Professor of MS research.

Accepted for publication March 26, 2009.

A guest editor acted as editor-in-chief for this manuscript. No person at Thomas Jefferson University or Albert Einstein College of Medicine was involved in the peer review process or final disposition for this article.

Address reprint requests to Dr. Bridget Shafit-Zagardo, Department of Pathology, Forchheimer 516S, Albert Einstein College of Medicine, 1300 Morris Park Avenue, Bronx, NY 10461. E-mail: zagardo@aecom.yu.edu.

We previously reported mRNA expression of Axl, Tyro3, and Mer receptors on human fetal oligodendrocytes and the ability of Gas6 to promote oligodendrocyte survival *in vitro* by activating Axl, resulting in Axl directly and indirectly recruiting phosphatidylinositol 3 kinase and activating the Akt pathway.[19,20] Moreover, we have shown that Gas6/Axl signaling through the Akt pathway can protect oligodendrocytes from tumor necrosis factor α (TNFα)-induced apoptosis.[21] Down-regulation or deletion of Axl, even in the presence of Gas6, results in loss of protection against TNFα.[22]

During the relapse phase of relapsing-remitting MS, serum TNFα levels and TNFα mRNA are elevated.[23,24] TNFα is one of the major cytokines expressed in MS lesions.[25] TNFα is cleaved to its mature, soluble, secretable form by the matrix metalloproteinase (MMP) TNFα converting enzyme, also known as ADAM17.[26–28] MMPs, including ADAM17 and ADAM10 are involved in normal processes such as wound repair and tissue remodeling and are associated with disease states, including MS.[29–36] Expression of ADAM17 is observed in acute and chronic active MS lesions, primarily in perivascular cuffs and cells morphologically resembling lymphocytes.[37] ADAM17 up-regulation in cerebrospinal fluid of MS patients is associated with inflammation and increased soluble TNFα.[37,38] ADAM10 is constitutively expressed on astrocytes in normal appearing white matter and on astrocytes and perivascular macrophages in MS lesions.[38–41] ADAM10 cleaves Axl, and ADAM17 cleaves Axl and Mer. Cleaved forms of receptors can result in internalization of the receptor and transport off the membrane for recycling. Cleavage can also result in shortened, soluble forms that act as a decoy to regulate the level of a growth factor at the membrane.[41,42]

Soluble forms of Axl and Mer can reduce the number of viable receptors for Gas6 binding and act as a decoy by sequestering Gas6 extracellularly; potentially a normal mechanism of receptor activation regulation.[40,41] During inflammation, soluble Mer has been reported to inhibit macrophage clearance of apoptotic cells.[41,43] Also, soluble Axl blocked the protective effect of membrane-bound Axl by inhibiting Gas6 induced tyrosine phosphorylation of Axl.[44] The binding of Gas6 to TAM receptors acts as an inhibitor of inflammation by inhibiting Toll-like receptor and cytokine receptor cascades.[44] Up-regulation of Axl and its subsequent interaction with interferon α and β receptors results in the expression of cytokine and Toll-like receptor inhibitors.[44,45] Thus, loss of Gas6 signaling, along with dysregulation of the balance between Gas6, Axl and Mer by increased extracellular levels of soluble Axl and Mer, might detrimentally impact the nervous system, especially in established (chronic active and chronic silent) lesions associated with MS. Chronic active MS lesions are characterized by ongoing demyelination, astrogliosis, macrophage and lymphocyte infiltration, astroglial hypertrophy, and oligodendrocyte hyperplasia.[46] Chronic silent MS lesions are characterized by the absence of actively infiltrating and inflammatory cells, oligodendrocyte loss and no evidence of ongoing demyelination.[46,47,48]

In this study, we investigated in chronic active and chronic silent MS lesions whether increased expression of soluble Axl and Mer was associated with increased expression of the MMPs ADAM17 and ADAM10, similar to previous studies that showed an association between increased ADAM17 and ADAM10 with TNFα in the CNS of MS patients.[37,38] We also investigated whether in lesions increased soluble Axl and Mer was associated with decreased Gas6, resulting in loss of the beneficial effects from activating membrane-bound Axl and Mer receptors.

Materials and Methods

Human Tissue Samples

Cryostat sections and protein homogenates were prepared from nine MS cases; two primary progressive and seven secondary progressive, in total containing six chronic active and eight chronic silent lesions. Tissue sections and homogenates from cerebral white matter of three cases of other neurological disease (OND) included olivopontocerebellar degeneration, amyotrophic lateral sclerosis, and stroke. Tissue from three non-neurological subjects, and

Table 1. Summary of Cases Utilized for Immunohistochemistry and Immunoblotting

Case no.	Diagnosis	Disease duration (yr)	Sex/age (yr)	Cause of death
1	PPMS	8	F/31	Respiratory failure
2	PPMS	20	F/39	Respiratory failure
3	SPMS	11	F/38	Bronchopneumonia
4	SPMS	20	F/45	Bronchopneumonia
5	SPMS	20	F/47	Cardiac arrest
6	SPMS	21	F/56	Cardiac arrest
7	SPMS	15	M/46	Cardiac arrest
8	SPMS	23	M/67	Cardiac arrest
9	SPMS	16	M/61	Cardiac arrest
10	OPCD	4	M/31	Bronchopneumonia
11	ALS	5	F/49	Bronchopneumonia
12	Stroke	12 hours	F/80	Stroke
13	Non-neurological	n/a	M/19	Cardiac arrest/obesity
14	Non-neurological	n/a	M/40	Adult respiratory distress
15	Non-neurological	n/a	F/80	Metastatic cancer

PPMS, primary progressive multiple sclerosis; SPMS, secondary progressive multiple sclerosis; OPCD, olivopontocerebellar degeneration; ALS, amyotrophic lateral sclerosis; n/a, not applicable.

five normal appearing white matter sections from MS brains were classified as normal (Table 1). There were no histological differences between tissue from non-neurological subjects and normal appearing white matter; therefore, material from these subjects were grouped.

Immunohistochemistry

Ten-micrometer frozen sections fixed in acetone were quenched for endogenous peroxidase activity and blocked for 1 hour with 10% normal goat serum. Sections were then incubated with primary antibodies against Gas6 (catalog AF885), Axl (MAB154), Mer (MAB8911), and Tyro3 (MAB859; R&D Systems; Minneapolis, MN) or Gas6 polyclonal antibody (generated in the laboratory of Dr. Anne Prieto, Indiana University), diluted in 2% normal goat serum in 1X Tris-buffered saline (TBS) overnight at 4°C. Immunoreacted sections were developed by incubating with biotinylated secondary antibodies, followed by Vectastain avidin-biotin complex solution (Vector Laboratories; Burlingame, CA), and 3,3′-diaminobenzidine (DAB) solution (KPL, Gaithersburg, MD). As negative controls, sections were incubated with isotype-matched irrelevant antibodies (BD Bioscience; San Diego, CA), at the same concentration as the primary antibody, or with carrier buffer alone.

Double-label immunohistochemistry was performed to confirm the identity of the cells expressing Axl. Sections were stained with the Axl primary antibody and developed with DAB as described above. Sections were then washed twice with 1X TBS, permeabilized in 0.25% Triton X-100 in 1X TBS for 30 minutes at 22°C, washed an additional two times with 1X TBS, and incubated with the astrocyte specific marker, glial fibrillary acidic protein (1:300; Biogenex; San Ramon, CA) polyclonal antibody (pAb) or the microglia specific marker, Iba-1 (1:400, Wako; Richmond, VA) pAb in 1X TBS plus 5% bovine serum albumin, overnight at 4°C. Alternatively, after development with DAB and subsequent washes, sections were incubated with 10 μg/ml Proteinase K (Sigma, Saint Louis, MO) in 20 mmol/L Tris pH 7.5 for 15 minutes at 37°C; washed in 0.1% Triton X-100 in 1X TBS for 30 minutes at 22°C; and blocked in 5% goat serum/0.1% Triton X-100/5% milk in 1X TBS for 1 hour at 22°C. These alternatively treated sections were incubated with the oligodendrocyte-specific marker, platelet-derived growth factor receptor α (PDGFRα, 1:100) overnight at 4°C. The PDGFRα pAb was generated in the laboratory of Dr. William Stallcup at the Burnham Institute for Medical Research (La Jolla, CA). Following incubation with primary antibodies, the sections were washed three times in 1X TBS and incubated with alkaline phosphatase (AP)-conjugated goat anti-rabbit secondary antibody (1:300; Southern Biotechnology; Birmingham, AL), for 1 hour at 22°C. One Sigma Fast 5-bromo-4-chloro-3-indolyl phosphate/nitro blue tetrazolium AP (BCIP/NB-AP) substrate tablet (Sigma) was dissolved in 10 ml of ddH_20 (plus 1 μmol/liter levimasole (Sigma)). Sections were incubated with BCIP/NB-AP for 30 minutes at 22°C, washed three times with 1X TBS, dehydrated in 80%/95%/100% ethanol for 5 minutes each, followed by xylene for 10 minutes, and mounted under Permount (Fisher Scientific; Fair Lawn, NJ).

Western Blot Analysis

Total protein was extracted from fresh frozen brain autopsy tissue from chronic active MS, chronic silent MS, OND, and normal cases as previously described. Except where noted in the figure legends, 80 μg of protein were loaded in 1X final concentration loading buffer containing 2% sodium dodecyl sulfate, 0.017% bromophenol blue dye, and 0.28 mol/L β-mercaptoethanol (load dye) and separated in a 10% sodium dodecyl sulfate-polyacrylamide gel by electrophoresis.[49,50,51] Following electrophoresis, proteins were transferred to nitrocellulose. Blots were incubated with 5% nonfat dry milk and 5% goat serum in 1X TBS for 1 hour at room temperature. After blocking, membranes were incubated with respective primary antibodies followed by horseradish peroxidase-conjugated secondary antibodies. Primary monoclonal antibodies (mAb) and pAb's included: Axl mAb (IgG1, 1:250), Tyro3 mAb (IgG1, 1:500), Mer mAb (IgG2b, 1:500), R&D Gas6 pAb (1:100), Prieto Gas6 pAb (1:8000), Furin pAb (1:250, made in the laboratory of Dr. Dennis Shields, Albert Einstein College of Medicine), ADAM10 pAb (1:1000, eBioscience; San Diego, CA), ADAM17 pAb (1:1000, eBioscience), and β-actin mAb (IgG2A, 1:5000; Sigma, St. Louis, MO). Secondary antibodies (Jackson ImmunoResearch Laboratories; West Grove, PA) included: goat α-rabbit IgG (1:10,000), and goat α-mouse IgG1 (1:10,000), IgG2A (1:10,000), and IgG2b (1:10,000). Visualization of all secondary antibodies was by enhanced chemiluminescence (GE HealthCare; Piscataway, NJ).

Glycosylation Assay

A peptide-*N*-glycosidase F (PNGaseF) kit (QAbio; Palm Desert, CA) was used to assess glycosylation of ADAM17. The volume of 40 μg of protein homogenate from normal samples was adjusted to 35 μl, and 10 μl of 5 $\times$ 250 mmol/L sodium phosphate, pH 7.5 (reaction buffer), and 2.5 μl of 2% sodium dodecyl sulfate, 1 mol/L β-mercaptoethanol (denaturation solution) were added. Samples were heated at 100°C for 5 minutes, cooled on ice, and 2.5 μl of 0.1% Triton X-100 and 2 μl of PNGaseF (5 U/ml in 20 mmol/L Tris-HCl, pH 7.5) were added. Samples were incubated for 3 hours at 37°C. For control purposes, a protein homogenate was used that was treated and incubated as described above except no PNGaseF was added. All samples were separated in a 10% sodium dodecyl sulfate gel by polyacrylamide gel electrophoresis, transferred to nitrocellulose, and Western blot analysis for ADAM17 was performed as previously described.

Densitometry and Statistical Analysis

Autoradiographs were scanned in an Epson perfection 1200U flatbed scanner at 600 dpi. Densitometry was performed on scanned images in ImageJ (image processing program developed at the NIH), by measuring the mean gray value and the area for each band. A background measurement was also taken. Mean gray

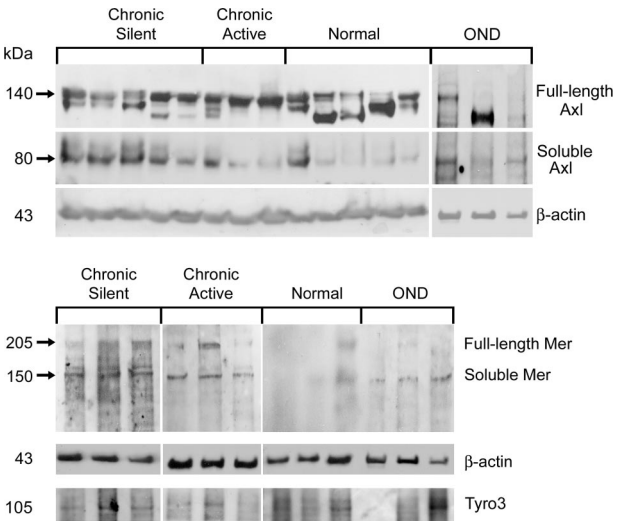

Figure 1. Full-length and soluble Axl, Mer, and Tyro3 expression in brain tissue homogenates. Western blot analysis was performed using Axl, Mer, and Tyro3 mAbs on 80 μg of chronic active, OND, normal, and chronic silent brain tissue homogenates. The Axl and Mer mAb's bind full-length and soluble forms of Axl and Mer, respectively. Six to eight samples were tested for each group except OND, where $n = 3$ for all antibodies tested except Tyro3 ($n = 2$). β-Actin was used as a loading control.

values were subtracted from background and multiplied by band area. Band values were normalized to actin (also measured as described above), to obtain the relative densitometric intensity. Student's *t*-tests were performed on normal versus chronic active, and normal versus chronic silent relative densitometric intensity for each antibody tested. Correlation coefficients were calculated in Microsoft Excel. Correlation coefficient ratings were based on a modification of the Cohen scale for interpreting correlation coefficients.[52]

Results

Soluble Axl and Mer Are Elevated in Established MS Lesions

Protein homogenates isolated from chronic active and chronic silent MS lesions, ONDs, and non-neurologically diseased CNS tissue were examined by Western blot analysis. There was no statistically significant difference between full-length Axl or Tyro3 from normal tissue ($n = 8$), chronic active lesions ($n = 6$), and chronic silent lesions ($n = 8$). Although full-length Axl was not significantly different in established lesions, soluble Axl was significantly higher in chronic silent lesions than normal tissue (4.2-fold; $P < 0.01$). Despite a 2.6-fold increase relative to normal homogenates, soluble Axl was not significantly different in chronic active lesion homogenates, due to variability of soluble Axl among chronic active lesion samples (Figures 1 and 2,A and D). Expression of soluble Axl in normal brain homogenates was low in all samples except one. Further, soluble Mer was detected at very low levels in normal tissue and was significantly elevated in chronic active (3.1-fold; $P < 0.05$) but not chronic silent lesions, despite a 2.3-fold increase (Figures 1, 2, B and E, and 3). Soluble Tyro3 was not detected in any brain homogenates (Figure 2C). There was no increase of any of the full-length or soluble receptors in OND tissue relative to normal.

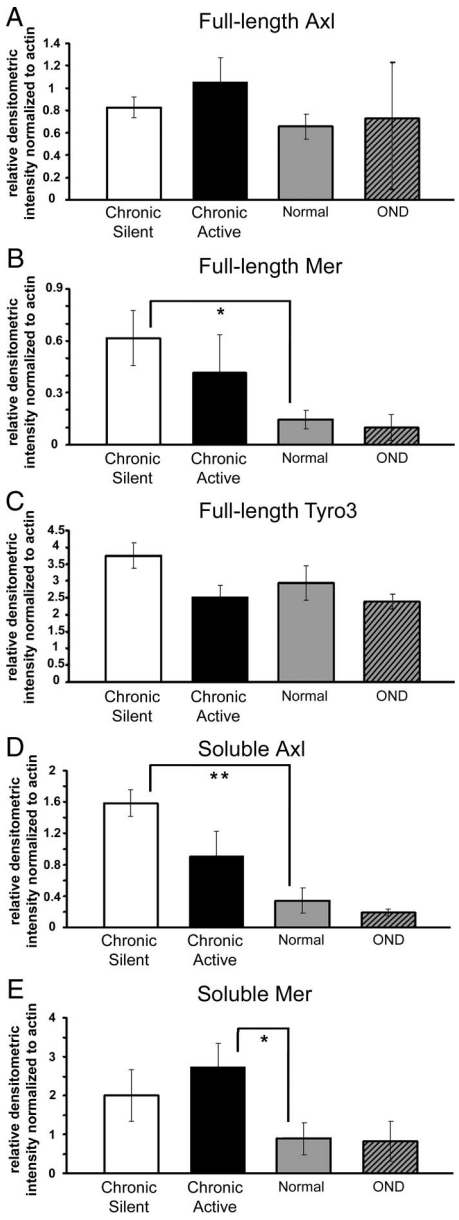

Figure 2. Relative to normal homogenates, soluble Axl is significantly increased in chronic silent tissue homogenates, soluble Mer is significantly increased in chronic active, and full-length Mer is significantly increased in chronic silent tissue homogenates. **A–E:** The relative densitometric intensity was determined for each band and normalized to β-actin. Average values for full-length Axl (**A**), Mer (**B**), and Tyro3 (**C**), and average values for soluble Axl (**D**) and Mer (**E**) in chronic active, OND, normal, and chronic silent brain tissue homogenates are shown. Significance was tested by Student's *t*-test between chronic active or chronic silent, and normal tissue homogenates; $^{*}P < 0.05$, $^{**}P < 0.01$.

Axl and Mer Are Elevated on Glial Cells in Established MS Lesions

Immunohistochemistry was performed to identify cell types expressing elevated Axl and Mer, and to verify

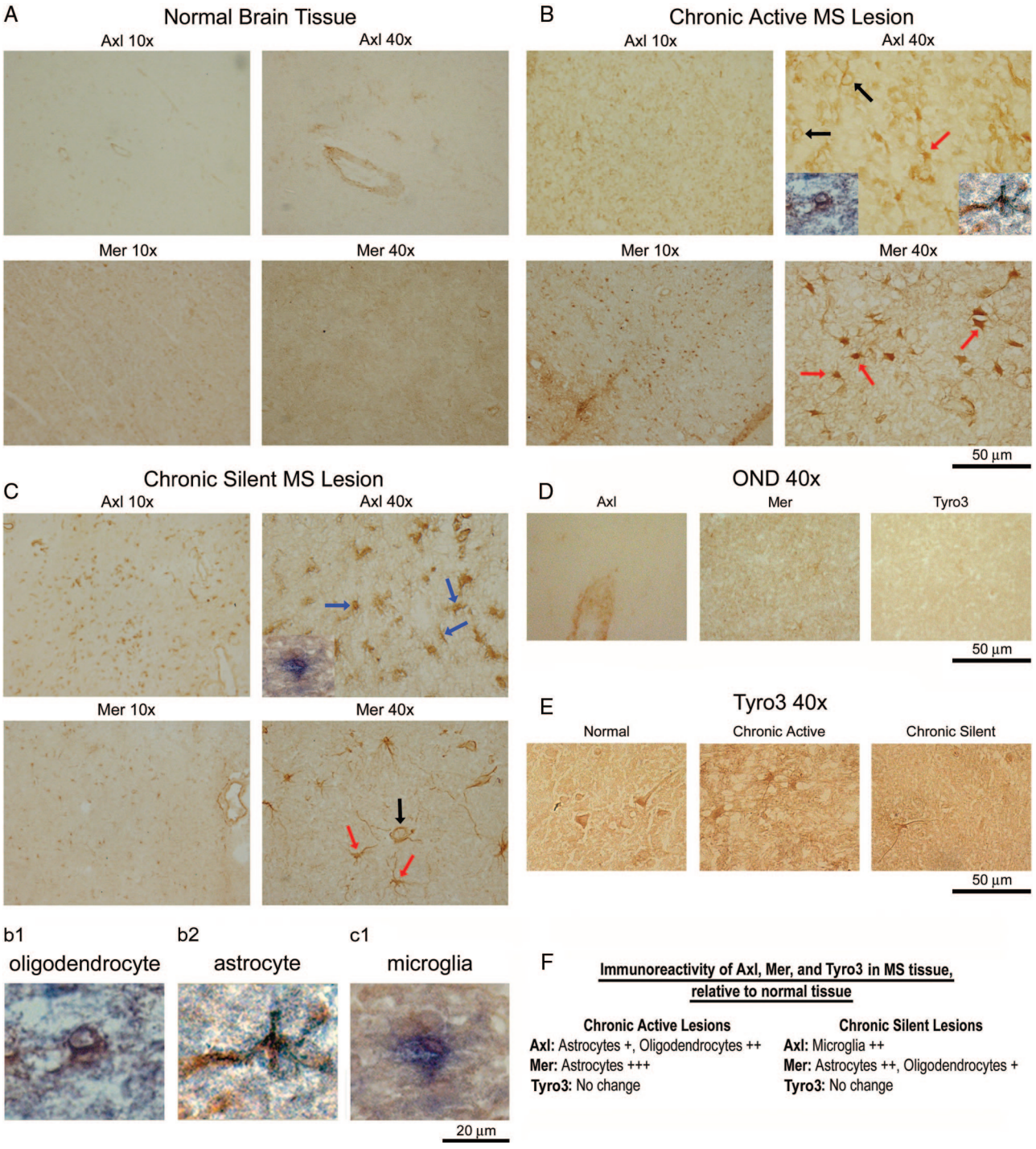

Figure 3. Altered Axl and Mer immunoreactivity in sections of chronic active and chronic silent MS lesions. Ten-micrometer frozen sections were stained with Axl, Mer and Tyro3 (**E**) mAbs. Staining of normal brain (**A**), chronic active (**B**), chronic silent (**C**) MS lesions, and OND (**D**) samples were visualized by DAB. Representative 10X and 40X images are shown. Magnification, 50-μm bar = ×40. **Red arrows** point to astrocytes (**B** and **C**), **blue arrows** to microglia (**C**), and **black arrows** to oligodendrocytes (**B** and **C**). To verify cell morphology, double-label immunohistochemistry was performed with an Axl mAb using a biotinylated secondary antibody with DAB and a PDGFRα pAb for oligodendrocytes (**B**, chronic active Axl 40X, **left inset,** and **b1**), glial fibrillary acidic protein pAb for astrocytes (**B**, chronic active Axl 40X, **right inset**, and **b2**), or Iba-1 pAb for microglia (**C**, chronic silent Axl 40X, **left inset**, and **c1**) using an AP secondary antibody with BCIP/NB-AP. The **b1**, **b2**, and **c1 insets** are enlarged to better show overlapping co-staining of DAB and AP. **F:** Axl and Mer were semiquantitatively evaluated in chronic active and chronic silent lesions and were scored relative to expression of each receptor in normal brain tissue on a 1–3+ scale. Moderate increase was rated +, high increase was rated ++, and very high increase was rated +++.

Western blot data. Sections from brains of primary progressive and secondary progressive MS patients and non-neurological controls were incubated with Axl, Mer, and Tyro3 antibodies. There was low level expression of both Axl and Mer in normal brain tissue (Figure 3A). Axl expression was elevated on astrocytes and oligodendrocytes in chronic active lesions, as determined by morphology and verified by double- label immunohis-

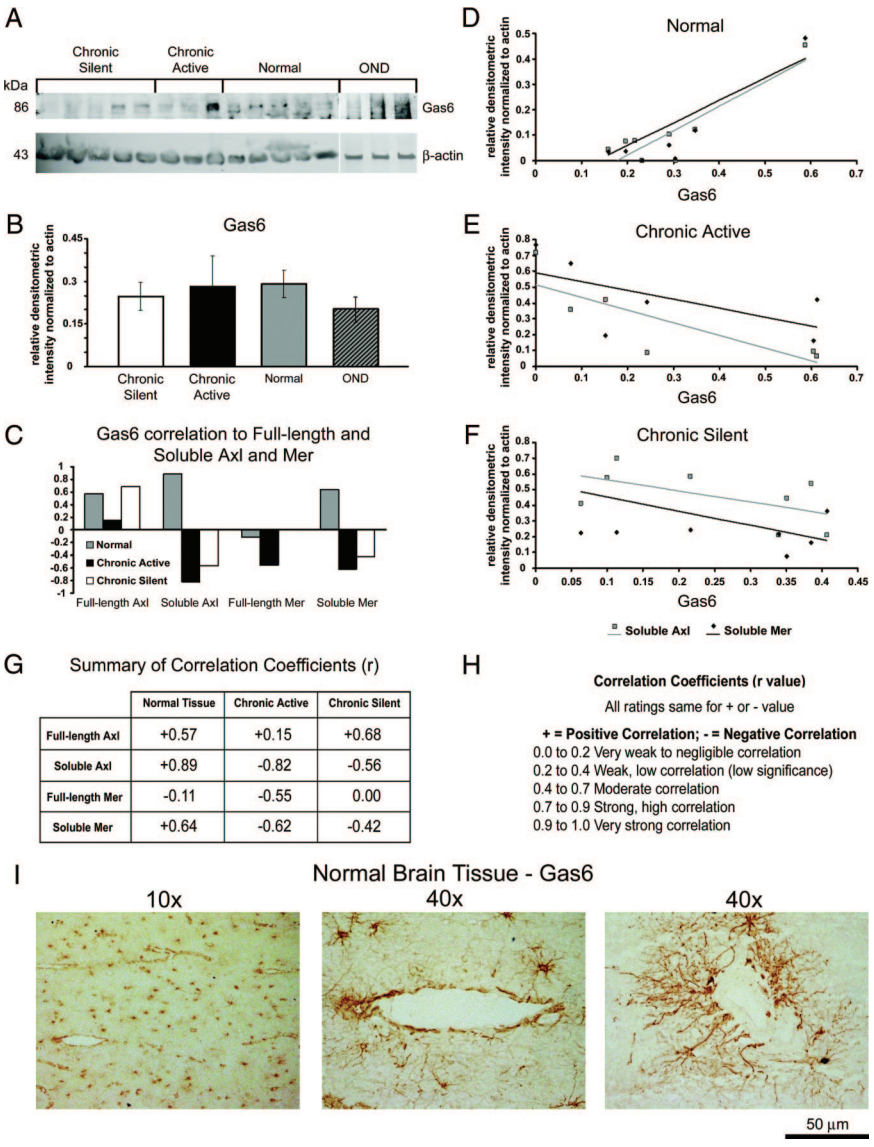

	Normal Tissue	Chronic Active	Chronic Silent
Full-length Axl	+0.57	+0.15	+0.68
Soluble Axl	+0.89	-0.82	-0.56
Full-length Mer	-0.11	-0.55	0.00
Soluble Mer	+0.64	-0.62	-0.42

Figure 4. Negative correlation coefficients between Gas6 expression relative to soluble Axl and Mer in chronic active and chronic silent tissue homogenates. **A:** Blots containing 80 μg of chronic active, OND, normal, and chronic silent brain tissue homogenates were incubated with a Gas6 pAb. β-Actin was used as a loading control. **B:** The relative densitometric intensity was determined for each band normalized to β-actin and the average value for Gas6 in chronic active, OND, normal, and chronic silent brain tissue homogenates are shown. **C:** Correlation coefficients (r) were calculated between Gas6 and full-length and soluble Axl and Mer in normal, chronic active, and chronic silent brain tissue homogenates. **D–F:** Relative densitometric intensity for soluble Axl and Mer were graphed versus relative densitometric intensity for Gas6 for normal (**D**), chronic active (**E**), and chronic silent (**F**). Values for soluble Axl and Mer were normalized to use a linear scale for the x axis. A positive slope of the trend line indicates a positive correlation and a negative slope indicates a negative correlation with Gas6. **G:** Summary of correlation coefficients. **H:** Ratings of correlation coefficient values on scale from -1 to $+1$ based on a modification of the Cohen scale for interpreting correlation coefficients. **I:** Ten-micrometer frozen normal white matter brain tissue sections are stained with Gas6 pAb and visualized by DAB. Representative 10X and 40X images are shown. **Left** 40X image is high magnification of 10X image and **right** 40X image is from another normal brain tissue section. Magnification, 50-μm bar = $\times$40.

tochemistry with Axl (DAB) and PDGFα (AP; Figure 3B, bottom left inset of Axl 40X, and b1), or glial fibrillary acidic protein (AP; bottom right inset of Axl 40X, and b2). Mer expression was elevated on astrocytes in chronic active lesions (Figure 3B). In chronic silent lesions, Axl was elevated on microglia, morphologically verified by double labeling with Axl (DAB) and Iba-1 (AP; Figure 3C, bottom left inset of the Axl 40X, and c1). Mer expression was elevated on astrocytes and oligodendrocytes in chronic silent lesions (Figure 3C). Consistently, no difference in OND samples (Figure 3D) for Axl, Mer, or Tyro3 immunoreactivity relative to normal tissue was detected. In addition, there was no difference in Tyro3 immunoreactivity in chronic active or chronic silent tissue (Figure 3E). Semiquantitatively evaluated expression ratings for each receptor from chronic active and chronic silent lesions are shown in Figure 3F.

High Levels of Soluble Axl and Mer Correlate with Low Levels of Gas6 in Established MS Lesions

It is well established that Gas6 binds to and activates Axl, Mer, and Tyro3; however, it is not known whether Gas6 levels increase or decrease in response to elevated soluble forms of Axl and Mer within MS lesions. Western blot (Figure 4A) and densitometric analysis (Figure 4B) determined that when normalized to β-actin, there was no statistically significant change in Gas6 (86 kd). Calculation of correlation coefficients (r) between Gas6 and soluble Axl and Mer (Figure 4C) showed that in normal tissue homogenates, Gas6 positively correlated with soluble Axl ($r = 0.89$) and soluble Mer ($r = 0.64$). A summary of the correlation coefficients and ratings is shown in Figure 4, G and H. In chronic active lesions, Gas6 negatively correlated with soluble Axl ($r = 0.82$) and soluble

Mer ($r = -0.62$). In addition, in chronic silent lesions, Gas6 expression negatively correlated with soluble Axl ($r = -0.56$) and soluble Mer ($r = -0.87$). A graphical representation of the relationship between Gas6 and soluble Axl and Mer is shown in Figure 4, D–F. A positive slope (m) indicates a positive correlation between Gas6 and either soluble Axl or Mer while a negative slope indicates a negative correlation. In normal tissue, when Gas6 (x axis) was expressed at low levels, so were soluble Axl ($m = 0.96$) and Mer ($m = 0.88$); however, when Gas6 was expressed at high levels, soluble Axl and Mer were also highly expressed (Figure 4D). Conversely, in chronic active (Fig. 4E) and chronic silent (Fig. 4F) tissue, low expression of Gas6 corresponded to high expression of soluble Axl (chronic active $m = -0.80$, chronic silent $m = -0.70$) and Mer (chronic active $m = -0.56$, chronic silent $m = -0.90$). These data showed that within an MS lesion, the balance between Gas6 and soluble Axl and Mer was altered relative to normal tissue.

Immunohistochemical analysis determined and we report here for the first time that Gas6 is expressed on astrocyte cell bodies, processes, and end feet, as well as on vessels within the normal CNS (Figure 4I). High magnification (40×) clearly show the astrocytic processes extending to the end feet along the vessels. Although there appeared to be less Gas6 on astrocytes within the MS lesion tissue, overall expression was highly variable (data not shown), similar to the Western blot data.

Expression of Regulators of Axl and Mer Solubilization Is Altered in Established MS Lesions

After determining that a negative correlation between Gas6 and soluble Axl and Mer existed in MS lesion homogenates, we evaluated levels of ADAM17 and ADAM10, MMPs involved in regulation of Axl and Mer solubilization. The major ADAM17 forms are reported to migrate as an immature doublet at ~130 kd, and a mature doublet of ~100 kd. The difference observed in the mature doublet is a result of glycosylation.[53] As part of our analysis, we evaluated whether the relative expression of mature ADAM17 differed in established lesions. All densitometric values were normalized to β-actin. Western blot and densitometric analysis of ADAM17 was performed on MS, OND and neurologically-normal brain homogenates (Figure 5). At ~100 kd, two mature ADAM17 bands were observed (Figure 5A). To verify that the mature ADAM17 doublet was the result of altered glycosylation, protein homogenate from normal tissue was incubated with PNGaseF. When the protein homogenate was treated with PNGaseF, the mature 100-kd ADAM17 doublet migrated as a lower single band with a molecular weight of approximately 80 kd (Figure 5B). When mature 100-kd ADAM17 doublet bands were combined and normalized to β-actin, there were significantly more total mature ADAM17 in chronic active tissue relative to normal (Figure 5C).

Western blot and densitometric analysis for ADAM10 was performed on MS, OND, and normal brain homogenates. Immature ADAM10 migrated as a single band at ~85 kd and mature ADAM10 migrated at ~60 kd (Figure 6A). Relative to normal tissue, full-length immature ADAM10 was not significantly increased in established lesions (Figure 6B). There were minimal to undetectable amounts of mature ADAM10 in normal tissue homogenates (Figure 6C). Mature ADAM10 was significantly elevated in chronic active and chronic silent lesions ($P < 0.01$; Figure 6C).

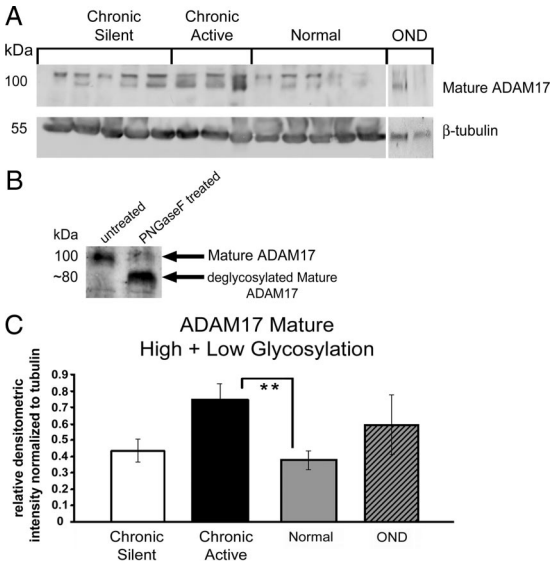

Figure 5. Relative to normal homogenates, mature ADAM17 is increased in chronic active tissue homogenates. **A:** Western blot analysis was performed using an ADAM17 pAb on 80 μg of chronic active, OND, normal, and chronic silent brain tissue homogenates. β-Actin was used as a load control. The ADAM17 pAb binds all forms of ADAM17. **B:** Before loading samples on gel, a normal brain homogenate sample (40 μg) was untreated (left lane) or treated with PNGaseF at 37°C for 3 hours. All other conditions were the same. The protein homogenates were analyzed by Western blot for glycosylation variants of mature ADAM17, using the ADAM17 pAb as in **A**. **C:** The relative densitometric intensity was determined for each band and normalized to β-actin. Data for the average values for mature ADAM17 (**C**) in chronic active, OND, normal, and chronic silent brain tissue homogenates are shown. Significance was tested between chronic active or chronic silent, and normal tissue homogenates; $^{**}P < 0.01$.

Since elevated Furin leads to increased mature ADAM10, we examined whether increase in mature ADAM10 in MS tissue might coincide with an increase in Furin. Densitometric analysis of Furin (Figure 7) in tissue homogenates from MS, OND, and normal brains showed Furin to be increased 4.2-fold in chronic active tissue and 1.4-fold in chronic silent tissue relative to normal tissue (Figure 7B). Levels of Furin strongly correlated with mature ADAM10 expression in chronic active ($r = 0.78$) tissue (Figure 7C).

Discussion

MS is a debilitating disease affecting the entire CNS. Elucidation of the many mechanisms and microenvironment changes that affect cell-cell interactions and signaling within a lesion resulting in cell death, demyelination and axonal damage is beneficial to understanding disease progression. Previously, we showed that the growth factor Gas6, through activation of its receptor, Axl, facil-

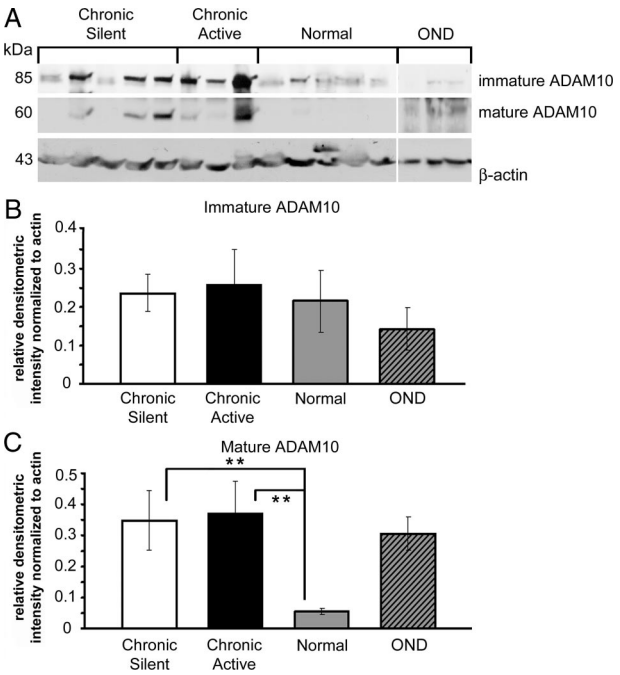

Figure 6. Mature ADAM10 is increased in chronic active and chronic silent tissue homogenates relative to normal. **A:** Western blot analysis was performed using an ADAM10 pAb on 80 μg of chronic active, OND, normal, and chronic silent brain tissue homogenates. Three samples were tested for each group. β-Actin was used as a loading control. The ADAM10 pAb binds immature and mature forms of ADAM10. The relative densitometric intensity was determined for each band and normalized to β-actin. **B** and **C:** The average values for immature ADAM10 (**B**) and mature ADAM10 (**C**) in chronic active, OND, normal, and chronic silent brain tissue homogenates are shown; $^{**}P < 0.01$. Different enhanced chemiluminescence exposure times are shown for immature and mature ADAM10 to best represent the data.

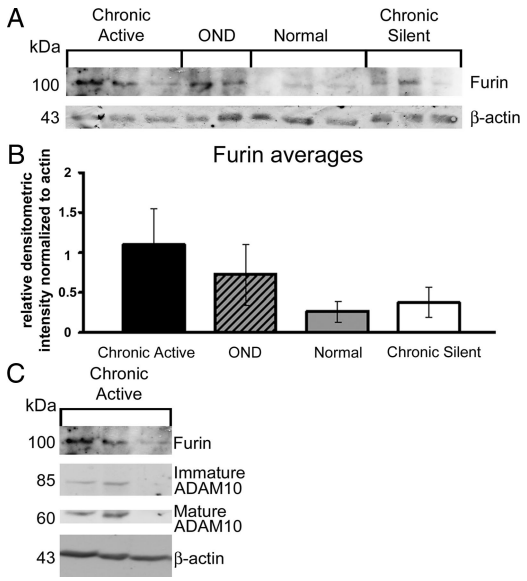

Figure 7. Increased Furin is detected in two of three chronic active homogenates relative to normal. **A:** Western blot analysis of chronic active, OND, normal, and chronic silent brain tissue homogenates was performed using a Furin. **B** and **C:** The relative densitometric intensity was determined for each band and normalized to β-actin. relative densitometric intensity data for the averages of Furin are shown in **B**. Corresponding chronic active samples stained with Furin, immature ADAM10 and mature ADAM10 are shown in **C** ($n = 3$ for all groups except OND for Furin, where $n = 2$).

itates oligodendrocyte survival. Using the cuprizone mouse model, we determined that mice with a deletion of Axl have a delay in recovery from cuprizone toxicity, indicating that Axl has an important role in normal CNS function. After 4 weeks cuprizone administration, the corpora callosa of *Axl−/−* mice display more apoptotic mature oligodendrocytes, and less clearance of apoptotic oligodendrocytes and myelin debris than wild-type mice. Wild-type mice recover by 3 weeks post-cuprizone withdrawal, while the *Axl−/−* mice have a delay in oligodendrocyte maturation and prolonged axonal damage.[54]

Following cuprizone administration, Gas6−/− mice have fewer mature oligodendrocytes, further underscoring the importance of the Gas6/Axl signaling pathway in oligodendrocyte survival.[55] In addition, Mer signals to induce clearance of debris by macrophages, an important function within an MS lesion.[42,44,56,57] Thus, loss or inhibition of Gas6, or dysregulation of Axl and Mer may contribute to the pathology observed in MS lesions.

We observed changes in Mer and Axl in protein homogenates from MS lesion tissue. Although there was no difference in full-length Axl between MS lesion and normal tissue, soluble Axl was expressed in all chronic active lesions and highly expressed in three of six. Soluble Axl was significantly elevated in chronic silent lesion samples ($P < 0.01$). In normal tissue homogenates there was minimal to undetectable expression in seven of eight samples. Full-length Mer was significantly increased in chronic silent lesion ($P < 0.05$) homogenates and soluble Mer was significantly elevated in chronic active ($P < 0.01$) tissue. Despite the quantified increase in soluble Axl and Mer, full-length Axl and Mer were not decreased in established MS lesions. Further, full-length Mer was significantly increased in chronic silent lesions and elevated, albeit not significantly, in chronic active lesions, suggesting either more full-length Axl and Mer were being synthesized or more full-length Axl and Mer were being introduced into the lesion via infiltrating or proliferating cells. It is also possible that more full-length Axl is converted to a mature 140-kd glycosylated form.[41] This would explain the presence of lower bands (<140 kd) in the normal and OND samples.

If indeed the membrane-bound receptors were not depleted but there was an increase in soluble forms of Axl and Mer, it is plausible that beneficial effects of Gas6 binding membrane-bound full-length Axl and Mer were blocked by soluble Axl and Mer acting as decoy receptors, thereby sequestering Gas6. We considered whether the high expression of soluble Axl and Mer correlated with low levels of Gas6. The two chronic active samples that had the most soluble Axl and soluble Mer had little to no Gas6 expression by immunoblotting. It is not known if low expression of Gas6 was due to extracellular Gas6 being targeted for degradation and/or removal or less Gas6 was being secreted relative to the amount of full-length Axl and Mer receptors. Less Gas6 being secreted and present in the lesion may be due to a change in cellular signaling as a result of severed or dying axons, or as a result of a change in the balance of Gas6-secreting cells.[58] In chronic silent tissue sections, there was little

change in amount of Gas6, yet there was an increase in expression of Axl and Mer on microglia, astrocytes, and oligodendrocyte progenitor cells. If there was no increase in Gas6 secretion, one would have expected an increase in inactivated full-length Axl and Mer receptors. The consequence of no concomitant Gas6 increase might be the solubilization of Axl and Mer by ADAM17 and ADAM10 in an attempt to eliminate the excess membrane-bound receptors and to restore the homeostatic ligand to receptor ratio. An imbalance between Gas6 and its receptors might explain the shift from a positive correlation in normal tissue, where soluble Axl and Mer increased with increased Gas6 expression, to a negative correlation, seen in MS lesion tissue homogenates.

Relative to normal tissue, mature ADAM17 was significantly increased in chronic active tissue. ADAM17 is the only known MMP to cleave Mer, and in chronic active lesions we observed a significant increase in both mature ADAM17 and soluble Mer. In addition to solubilizing Mer and Axl, ADAM17 is known to cleave and activate TNFα; both can lead to increased inflammation, loss of oligodendrocyte survival, loss of debris clearance, and more severe pathology in MS lesions.[39]

Mature ADAM10 was significantly elevated in chronic active and chronic silent tissue homogenates. *In vitro*, ADAM10 most efficiently cleaves Axl and therefore, is most likely to be the MMP responsible for cleaving Axl to its soluble form *in vivo*. Although we observed elevated ADAM17 and ADAM10 in OND, these samples did not have increased soluble Axl. This suggests that since ADAM17 and ADAM10 can cleave a multitude of proteins, such as EGF, βAPP, and CXCL16, the up-regulation of these MMPs in OND tissue is cleaving proteins [59–63] other than Axl and Mer. ADAM10 is cleaved and activated by Furin. By immunoblotting and densitometric analysis, Furin expression in two of three chronic active samples was increased over normal levels and coincided with the increase in mature ADAM10 observed in these chronic active MS samples. Increased maturation of ADAM10 was probably the result of increased Furin since there was no detectable increase in immature ADAM10. Conversely, in chronic silent tissue homogenates, there was an increase in mature ADAM10 in the absence of a concomitant increase in Furin. It is possible that a different mechanism for ADAM10 cleavage occurred in chronic silent lesions, perhaps by cleavage of another member of the nine-member family of convertases. It is also plausible that Furin was once elevated, responsible for the observed increase in mature ADAM10, then subsequently degraded. On the other hand, Furin activity within the chronic silent lesion may have been sufficient to cleave ADAM10 without further up-regulation.

Gas6 is known to enhance survival of oligodendrocytes, Schwann cells, and neurons *in vitro* and leads to reduced inflammation in animal models.[19,55,64–66] Our data have shown that in tissue homogenates prepared from MS lesions, there was negative correlation coefficient between Gas6 and soluble Axl and Mer that probably contributed to lesion pathology. Severed and degenerating axons, common features in active lesions, can contribute to diminished local Gas6 secretion and impact oligodendrocyte and axonal survival within lesions.[58] Hypercellularity within established lesions was associated with increased amounts of soluble Axl and Mer receptors. These abundant soluble receptors, known to sequester Gas6, may have limited the availability of free Gas6 to bind and activate membrane-bound receptors in the MS samples. Failure to properly activate membrane-bound Axl, Mer, and Tyro3 receptors can result in an inability to dampen the immune response, clear cell debris and protect CNS cells from damage, each of which would be important for remyelination to occur effectively. Future studies to determine the therapeutic potential of Gas6 to reduce deleterious effects of soluble Axl and Mer, may hold promise for the MS patient.

Acknowledgments

We thank Dr. Meng-Liang Zhao for reagents and help with alkaline phosphatase labeling. We thank Dr. William Stallcup at Burnham Institute for Medical Research for the PDGFRα pAb, Dr. Dennis Shields at Albert Einstein College of Medicine for the Furin pAb, and Dr. Anne L. Prieto at University of Indiana for the Gas6 pAb. We are grateful to Dr. Celia Brosnan for helpful comments and stimulating discussions. We thank Dr. Carol Petito, University of Miami Brain Bank (HD 83284), and Dr. Susan Morgello, Manhattan HIV Brain Bank (MH 59724), for providing normal CNS samples.

References

1. Sospedra M, Martin R: Immunology of multiple sclerosis. Annu Rev Immunol 2005, 23:683–747
2. Noseworthy JH, Lucchinetti C, Rodriguez M, Weinshenker BG: Multiple sclerosis. N Engl J Med 2000, 343:938–952
3. Fontoura P, Steinman L, Miller A: Emerging therapeutic targets in multiple sclerosis. Curr Opin Neurol 2006, 19:260–266
4. Frohman EM, Racke MK, Raine CS: Multiple sclerosis–the plaque and its pathogenesis. N Engl J Med 2006, 354:942–955
5. Raine CS: The Norton Lecture: a review of the oligodendrocyte in the multiple sclerosis lesion. J Neuroimmunol 1997, 77:135–152
6. Franklin RJ: Why does remyelination fail in multiple sclerosis? Nat Rev Neurosci 2002, 3:705–714
7. Prieto AL, Weber JL, Lai C: Expression of the receptor protein-tyrosine kinases Tyro-3. Axl, and mer in the developing rat central nervous system. J Comp Neurol 2000, 425:295–314
8. Stitt TN, Conn G, Gore M, Lai C, Bruno J, Radziejewski C, Mattsson K, Fisher J, Gies DR, Jones PF, Masiakowski P, Ryan TE, Tobkes NJ, Chen DH, DiStefano PS, Long GL, Basilico C, Goldfarb MP, Lemke G, Glass DL and Yancopoulos GD: The anticoagulation factor protein S and its relative: Gas6, are ligands for the Tyro 3/Axl family of receptor tyrosine kinases. Cell 1995, 80:661–670
9. Avanzi GC, Gallicchio M, Bottarel F, Gammaitoni L, Cavalloni G, Buonfiglio D, Bragardo M, Bellomo G, Albano E, Fantozzi R, Garbarino G, Varnum B, Aglietta M, Saglio G, Dianzani U, Dianzani C: GAS6 inhibits granulocyte adhesion to endothelial cells. Blood 1998, 91:2334–2340
10. Allen MP, Zeng C, Schneider K, Xiong X, Meintzer MK, Bellosta P, Basilico C, Varnum B, Heidenreich KA, Wierman ME: Growth arrest-specific gene 6 (Gas6)/adhesion related kinase (Ark) signaling promotes gonadotropin-releasing hormone neuronal survival via extracellular signal-regulated kinase (ERK) and Akt. Mol Endocrinol 1999, 13:191–201
11. Varnum BC, Young C, Elliott G, Garcia A, Bartley TD, Fridell YW, Hunt RW, Trail G, Clogston C, Toso RJ, Yanagihara D, Bennet L, Sylber M,

Merewether LA, Tseng A, Escobar E, Liu ET, Yamane HK: Axl receptor tyrosine kinase stimulated by the vitamin K-dependent protein encoded by growth-arrest-specific gene 6. Nature 1995, 373:623–626
12. Manfioletti G, Brancolini C, Avanzi G, Schneider C: The protein encoded by a growth arrest-specific gene (gas6) is a new member of the vitamin K-dependent proteins related to protein S, a negative coregulator in the blood coagulation cascade. Mol Cell Biol 1993, 13:4976–4985
13. Godowski PJ, Mark MR, Chen J, Sadick MD, Raab H, Hammonds RG: Reevaluation of the roles of protein S and Gas6 as ligands for the receptor tyrosine kinase Rse/Tyro 3. Cell 1995, 82:355–358
14. Chen J, Carey K, Godowski PJ: Identification of Gas6 as a ligand for Mer, a neural cell adhesion molecule related receptor tyrosine kinase implicated in cellular transformation. Oncogene 1997, 14:2033–2039
15. Nagata K, Ohashi K, Nakano T, Arita H, Zong C, Hanafusa H, Mizuno K: Identification of the product of growth arrest-specific gene 6 as a common ligand for Axl. Sky, and Mer receptor tyrosine kinases. J Biol Chem 1996, 271:30022–30027
16. Bellosta P, Costa M, Lin DA, Basilico C: The receptor tyrosine kinase ARK mediates cell aggregation by homophilic binding. Mol Cell Biol 1995, 15:614–625
17. Heiring C, Dahlback B, Muller YA: Ligand recognition and homophilic interactions in Tyro3: structural insights into the Axl/Tyro3 receptor tyrosine kinase family. J Biol Chem 2004, 279:6952–6958
18. Goruppi S, Ruaro E, Varnum B, Schneider C: Gas6-mediated survival in NIH3T3 cells activates stress signalling cascade and is independent of Ras. Oncogene 1999, 18:4224–4236
19. Shankar SL, O'Guin K, Cammer M, McMorris FA, Stitt TN, Basch RS, Varnum B, Shafit-Zagardo B: The growth arrest-specific gene product Gas6 promotes the survival of human oligodendrocytes via a phosphatidylinositol 3-kinase-dependent pathway. J Neurosci 2003, 23:4208–4218
20. Weinger JG, Gohari P, Yan Y, Backer JM, Varnum B, Shafit-Zagardo B: In brain, Axl recruits Grb2 and the p85 regulatory subunit of PI3 kinase; in vitro mutagenesis defines the requisite binding sites for downstream Akt activation. J Neurochem 2008, 106:134–146
21. Shankar SL, O'Guin K, Kim M, Varnum B, Lemke G, Brosnan CF, Shafit-Zagardo B: Gas6/Axl signaling activates the phosphatidylinositol 3-kinase/Akt1 survival pathway to protect oligodendrocytes from tumor necrosis factor alpha-induced apoptosis. J Neurosci 2006, 26:5638
22. Budagian V, Bulanova E, Orinska Z, Thon L, Mamat U, Bellosta P, Basilico C, Adam D, Paus R, Bulfone-Paus S: A promiscuous liaison between IL-15 receptor and Axl receptor tyrosine kinase in cell death control. EMBO J 2005, 24:4260–4270
23. Sharief MK, Hentges R: Association between tumor necrosis factor-alpha and disease progression in patients with multiple sclerosis. N Engl J Med 1991, 325:467–472
24. Bertolotto A, Malucchi S, Capobianco M, Manzardo E, Guastamacchia G, Milano E, Audano L, Mutani R: Quantitative PCR reveals increased levels of tumor necrosis factor-alpha mRNA in peripheral blood mononuclear cells of multiple sclerosis patients during relapses. J Interferon Cytokine Res 1999, 19:575–581
25. Perez C, Albert I, Defay K, Zachariades N, Gooding L, Kriegler M: A nonsecretable cell surface mutant of tumor necrosis factor (TNF) kills by cell-to-cell contact. Cell 1990, 63:251–258
26. Utsumi T, Levitan A, Hung MC, Klostergaard J: Effects of truncation of human pro-tumor necrosis factor transmembrane domain on cellular targeting. J Biol Chem 1993, 268:9511–9516
27. Moss ML, Jin SL, Becherer JD, Bickett DM, Burkhart W, Chen WJ, Hassler D, Leesnitzer MT, McGeehan G, Milla M, Moyer M, Rocque W, Seaton T, Schoenen F, Warner J, Willard D: Structural features and biochemical properties of TNF-alpha converting enzyme (TACE). J Neuroimmunol 1997, 72:127–129
28. Talhouk RS, Bissell MJ, Werb Z: Coordinated expression of extracellular matrix-degrading proteinases and their inhibitors regulates mammary epithelial function during involution. J Cell Biol 1992, 118:1271–1282
29. Jeffrey JJ: Collagen and collagenase: pregnancy and parturition. Semin Perinatol 1991, 15:118–126
30. Salamonsen LA: Matrix metalloproteinases and endometrial remodelling. Cell Biol Int 1994, 18:1139–1144
31. Stetler-Stevenson WG, Liotta LA, Kleiner DE Jr: Extracellular matrix 6: role of matrix metalloproteinases in tumor invasion and metastasis. FASEB J 1993, 7:1434–1441
32. Stetler-Stevenson WG, Aznavoorian S, Liotta LA: Tumor cell interactions with the extracellular matrix during invasion and metastasis. Annu Rev Cell Biol 1993, 9:541–573
33. Gijbels K, Galardy RE, Steinman L: Reversal of experimental autoimmune encephalomyelitis with a hydroxamate inhibitor of matrix metalloproteases. J Clin Invest 1994, 94:2177–2182
34. Matrisian LM: Metalloproteinases and their inhibitors in matrix remodeling. Trends Genet 1990, 6:121–125
35. Galis ZS, Sukhova GK, Kranzhofer R, Clark S, Libby P: Macrophage foam cells from experimental atheroma constitutively produce matrix-degrading proteinases. Proc Natl Acad Sci USA 1995, 92:402–406
36. Comabella M, Romera C, Camina M, Perkal H, Moro MA, Leza JC, Lizasoain I, Castillo M, Montalban X: TNF-alpha converting enzyme (TACE) protein expression in different clinical subtypes of multiple sclerosis. J Neurol 2006, 253:701–706
37. Kieseier BC, Pischel H, Neuen-Jacob E, Tourtellotte WW, Hartung HP: ADAM-10 and ADAM-17 in the inflamed human CNS. Glia 2003, 42:398–405
38. Guo L, Eisenman JR, Mahimkar RM, Peschon JJ, Paxton RJ, Black RA, Johnson RS: A proteomic approach for the identification of cell-surface proteins shed by metalloproteases. Mol Cell Proteomics 2002, 1:30–36
39. Budagian V, Bulanova E, Orinska Z, Duitman E, Brandt K, Ludwig A, Hartmann D, Lemke G, Saftig P, Bulfone-Paus S: Soluble Axl is generated by ADAM10-dependent cleavage and associates with Gas6 in mouse serum. Mol Cell Biol 2005, 25:9324–9339
40. Sather S, Kenyon KD, Lefkowitz JB, Liang X, Varnum BC, Henson PM, Graham DK: A soluble form of the Mer receptor tyrosine kinase inhibits macrophage clearance of apoptotic cells and platelet aggregation. Blood 2007, 109:1026–1033
41. O'Bryan JP, Fridell YW, Koski R, Varnum B, Liu ET: The transforming receptor tyrosine kinase. Axl, is post-translationally regulated by proteolytic cleavage. J Biol Chem 1995, 270:551–557
42. Scott RS, McMahon EJ, Pop SM, Reap EA, Caricchio R, Cohen PL, Earp HS, Matsushima GK: Phagocytosis and clearance of apoptotic cells is mediated by MER. Nature 2001, 411:207–211
43. D'Arcangelo D, Ambrosino V, Giannuzzo M, Gaetano C, Capogrossi MC: Axl receptor activation mediates laminar shear stress anti-apoptotic effects in human endothelial cells. Cardiovasc Res 2006, 71:754–763
44. Rothlin CV, Ghosh S, Zuniga EI, Oldstone MB, Lemke G: TAM receptors are pleiotropic inhibitors of the innate immune response. Cell 2007, 131:1124–1136
45. Sharif MN, Sosic D, Rothlin CV, Kelly E, Lemke G, Olson EN, Ivashkiv LB: Twist mediates suppression of inflammation by type I IFNs and Axl. J Exp Med 2006, 203:1891–1901
46. Raine CS: Multiple sclerosis: clinical and pathogenic basis. Edited by Raine CS, McFarland HF, Tourtellotte WW. Chapman & Hall Medical, 1997, pp 151–171
47. Lassmann H, Raine CS, Antel J, Prineas JW: Immunopathology of multiple sclerosis: report on an international meeting held at the Institute of Neurology of the University of Vienna. J Neuroimmunol 1998, 86:213–217
48. Cannella B, Raine CS: Multiple sclerosis: cytokine receptors on oligodendrocytes predict innate regulation. Ann Neurol 2004, 55:46–57
49. Laemmli UK: Cleavage of structural proteins during the assembly of the head of bacteriophage T4. Nature 1970, 227:680–685
50. Towbin H, Staehelin T, Gordon J: Electrophoretic transfer of proteins from polyacrylamide gels to nitrocellulose sheets: procedure and some applications. Proc Natl Acad Sci USA 1979, 76:4350–4354
51. Zamora-Leon SP, Bresnick A, Backer JM, Shafit-Zagardo B: Fyn phosphorylates human MAP-2c on tyrosine 67. J Biol Chem 2005, 280:1962–1970
52. Cohen J, Cohen P: Applied multiple regression correlation analysis for the behavioral sciences. 2nd edition. Hillsdale, New Jersey: L. Erlbaum Associates, 1983, pp 25–78
53. Endres K, Anders A, Kojro E, Gilbert S, Fahrenholz F, Postina R: Tumor necrosis factor-alpha converting enzyme is processed by proprotein-convertases to its mature form which is degraded upon phorbol ester stimulation. Eur J Biochem 2003, 270:2386–2393

54. Hoehn HJ, Kress Y, Sohn S, Brosnan C, Bourdon S, Shafit-Zagardo B: Axl-/-mice have delayed recovery and prolonged axonal damage following cuprizone toxicity. Brain Res 2008, 1240:1–11
55. Binder MD, Cate HS, Prieto AL, Kemper D, Butzkueven H, Gresle MM, Cipriani T, Jokubaitis VG, Carmeliet P, Kilpatrick TJ: Gas6 deficiency increases oligodendrocyte loss and microglial activation in response to cuprizone-induced demyelination. J Neurosci 2008, 28:5195–5206
56. Kotter MR, Zhao C, van Rooijen N, Franklin RJ: Macrophage-depletion induced impairment of experimental CNS remyelination is associated with a reduced oligodendrocyte progenitor cell response and altered growth factor expression. Neurobiol Dis 2005, 18:166–175
57. Zhao C, Fancy SP, Kotter MR, Li WW, Franklin RJ: Mechanisms of CNS remyelination the key to therapeutic advances. J Neurol Sci 2005, 233:87–91
58. Trapp BD, Peterson J, Ransohoff RM, Rudick R, Mork S, Bo L: Axonal transection in the lesions of multiple sclerosis. N Engl J Med 1998, 338:278–285
59. Abel S, Hundhausen C, Mentlein R, Schulte A, Berkhout TA, Broadway N, Hartmann D, Sedlacek R, Dietrich S, Muetze B, Schuster B, Kallen KJ, Saftig P, Rose-John S, Ludwig A: The transmembrane CXC-chemokine ligand 16 is induced by IFN-gamma and TNF-alpha and shed by the activity of the disintegrin-like metalloproteinase ADAM10. J Immunol 2004, 172:6362–6372
60. Kojro E, Gimpl G, Lammich S, Marz W, Fahrenholz F: Low cholesterol stimulates the nonamyloidogenic pathway by its effect on the alpha -secretase ADAM 10. Proc Natl Acad Sci USA 2001, 98:5815–5820
61. Lopez-Perez E, Zhang Y, Frank SJ, Creemers J, Seidah N, Checler F: Constitutive alpha-secretase cleavage of the beta-amyloid precursor protein in the furin-deficient LoVo cell line: involvement of the prohormone convertase 7 and the disintegrin metalloprotease ADAM10. J Neurochem 2001, 76:1532–1539
62. Sahin U, Weskamp G, Kelly K, Zhou HM, Higashiyama S, Peschon J, Hartmann D, Saftig P, Blobel CP: Distinct roles for ADAM10 and ADAM17 in ectodomain shedding of six EGFR ligands. J Cell Biol 2004, 164:769–779
63. Anders A, Gilbert S, Garten W, Postina R, Fahrenholz F: Regulation of the alpha-secretase ADAM10 by its prodomain and proprotein convertases. FASEB J 2001, 15:1837–1839
64. Yagami T, Ueda K, Asakura K, Sakaeda T, Nakazato H, Kuroda T, Hata S, Sakaguchi G, Itoh N, Nakano T, Kambayashi Y, Tsuzuki H: Gas6 rescues cortical neurons from amyloid beta protein-induced apoptosis. Neuropharmacology 2002, 43:1289–1296
65. Seitz HM, Camenisch TD, Lemke G, Earp HS, Matsushima GK: Macrophages and dendritic cells use different Axl/Mertk/Tyro3 receptors in clearance of apoptotic cells. J Immunol 2007, 178:5635–5642
66. Li R, Chen J, Hammonds G, Phillips H, Armanini M, Wood P, Bunge R, Godowski PJ, Sliwkowski MX, Mather JP: Identification of Gas6 as a growth factor for human Schwann cells. J Neurosci 1996, 16:2012–2019